Modeling and Numerical Simulation of Material Science, 2019, 9, 41-69
http://www.scirp.org/journal/mnsms
ISSN Online: 2164-5353
ISSN Print: 2164-5345

Tribological Behavior of Copper Chilled Aluminum Alloy (LM-13) Reinforced with Beryl Metal Matrix Composites

Joel Hemanth

School of Engineering, Presidency University, Bangalore, India
Email: joelhemanth@hotmail.com

How to cite this paper: Hemanth, J. (2019) Tribological Behavior of Copper Chilled Aluminum Alloy (LM-13) Reinforced with Beryl Metal Matrix Composites. *Modeling and Numerical Simulation of Material Science*, **9**, 41-69.
https://doi.org/10.4236/mnsms.2019.93004

Received: May 16, 2019
Accepted: July 20, 2019
Published: July 23, 2019

Abstract

The present investigation aims at developing copper chilled aluminum alloy (LM-13) reinforced with beryl using stir casting method. Matrix alloy was melted in a composite making furnace to a temperature of about 700˚C to which preheated reinforcement particles was added (3 wt.% to 12 wt.% in steps of 3 wt.%), stirred well and finally poured in to an AFS standard mold containing copper end chills of different thickness (10, 15, 20 and 25 mm) placed judiciously for directional solidification. The resulting chilled composites were subjected to microstructural, XRD, mechanical properties (strength and hardness) and tribological behavior. Results of the microstructural and XRD analysis indicate that the chilled castings were sound with good distribution and presence of all the particles. The bonding between beryl reinforcement and Al alloy matrix (LM-13) leads to excellent isotropic properties without any shrinkage or microporosity. Mechanical characterization indicates that both strength and hardness were maximum in the case of copper chilled MMC containing 9 wt.% and 12 wt.% reinforcement respectively. Strength and hardness of chilled MMC are found to increase by 9.88% and 16.66% as compared against the matrix alloy. It is observed that because of the ceramic (beryl) reinforcement in aluminum alloy, the wear resistance of the chilled composite developed has increased with increase in reinforcement content. At lower load, chilled MMCs exhibited mild wear regime with high coefficient of friction and at higher loads they exhibited severe wear with better wear resistance compared to un-chilled composite. It is observed that the increase in mechanical properties and wear resistance are due to incorporation of beryl reinforcement, the effect of chilling that has resulted in grain refined microstructure with good bonding of the matrix and the reinforcement.

Keywords

Aluminum, Beryl, Aluminum, Composite, Tribology

1. Introduction

Composite materials are the class of materials in which two phases are combined usually with strong interfaces between them. To improve the mechanical properties of bare aluminum alloys, aluminum composites materials came into existence viz. Metal Matrix Composites (MMCs), Polymer Matrix Composites (PMCs) and Ceramic Matrix Composites (CMCs). Nowadays in aerospace, marine and structural industries, aluminum-based composites materials are extensively used because of good mechanical properties (strength, hardness, toughness, density), tribological and corrosive behavior. Also, these composites are light in weight as compared with their strength and this significant weight reduction results in the material that fits for aerospace application in addition to fuel saving. Presently various aluminum alloy composites are being commonly used in which reinforcements may be in the form of fibers, flakes, whiskers, particulates, etc.

The main aim involved in designing the chilled metal matrix composites in the present investigation is to combine the desirable properties of aluminum alloy (LM-13) and ceramic reinforcement (beryl). The addition of reinforcement particles which possess high strength, hardness and high modulus to a ductile metal matrix results in a composite material whose mechanical properties are intermediate between the matrix alloy and ceramic reinforcements. Aluminum qualifies as the best matrix material due to its availability, cost and ease of fabrication. Of all the structural materials, aluminum is abundantly found in the earth's crust, and it is the third most abundant element after oxygen and silicon. Apart from ease of availability, aluminum also possesses desirable characteristics such as high strength to weight ratio, corrosion resistant, ease in machining, good durability with sufficient ductility. Aluminum is a very light metal with a specific weight of 2.7 gm/cc which is fit for aerospace applications. These characteristics have enabled the use of aluminum as the primary material of choice for automobile and aerospace applications. Aluminum alloys probably form the widely used matrix materials for MMCs since it is light in weight. Because of its advantage, metal matrix composite will replace conventional materials in many commercial and industrial applications. Al-based particulate reinforced MMCs which possess an excellent strength to weight ratio are attractive for practical applications like automobile, aerospace and defense industries. Toughness and formability of aluminum can be combined with strength and hardness of reinforcement on weight adjusted basis to outperform the conventional material.

Driven by the ever increasing demand for high strength, low weight materials and advancements in manufacturing technologies, the growth in the field of composites has been many fold. It goes without the saying that the technological advancements in the design and manufacturing of composite materials has fueled the growth of automobile and aerospace sector and has enabled various nations around the world to achieve the low cost spatial exploration. It was also that the ease with which the composites adapt themselves to the specific requirements has also contributed immensely to the popularity of composite ma-

terials. Hence, composite materials are tailor-made to meet specific requirements that have successfully overtaken the monolithic materials and find their presence in almost all fields.

It is well known that Al alloys that freeze over a wide range of temperature are difficult to feed during solidification. The dispersed porosity caused by the pasty mode of solidification can be effectively reduced by the use of chills. Chills extract heat at a faster rate and promote directional solidification. Therefore chills are widely used by foundry engineers for the production of sound and quality castings. There have been several investigations [1] [2] [3] [4] [5] on the influence of chills on the solidification and soundness of alloys. With the increase in the demand for quality composites, it has become essential to produce Al composites free from unsoundness.

Search of open literature indicates that so far no investigation has been done on microstructure, mechanical and tribological properties of Al-alloy (LM-13) and beryl chilled particulate MMCs and no detailed research is available on the tribological behavior of the same manufactured by chill casting technique. Hence the present investigation is undertaken to fill the void since this chilled MMC has great importance in aerospace as well as in the automobile sector. Thus, the current research work gives the state of the art on chill casting of beryl reinforced aluminum alloy matrix composites with regard to processing, microstructure, mechanical properties and tribological behavior.

2. Literature Review

Systematic study of the literature review indicated that 1990s belonged to era of aluminum metal matrix composites reinforced with particulate reinforcements in general and SiC in particular, the response of the MMC at elevated temperatures on parameters such as aging, ultimate tensile.

Strength and fatigue behavior also came under the study [6] [7] [8] [9] [10]. Titanium matrix composites began to evolve only during the late 1990s as researchers came up with specific applications for these materials in the field of aerospace.

During the late 1980s and early 1990s the research was focused mainly on aluminum and titanium matrix composites. This period saw the emergence of aluminum metal matrix composites cast with discontinuous reinforcements. This was due to massive funding by the US Air Force projects called Title-III. This has firmly laid the foundation for the development of numerous applications of composite materials employing discontinuously reinforced in aluminum matrix. The researchers around the world focused on developing lighter and stronger materials. Massive research on light weight metal matrix composites set forth, in which the leading matrix metal was aluminum followed by titanium to some extent. These matrices were reinforced by both continuous as well as discontinuous reinforcements. Powder reinforcements were added in high volume percentage to the metal matrices [11] [12] [13] [14] [15] and the composites thus developed were employed in electronic packaging which has required an excel-

lent thermal management [16]. Later there was a considerable shift from continuous reinforcement composites to discontinuous reinforcement composites and the success of discontinuously reinforced metal matrix composites through improved affordability and ease of process ability expanded the application areas of the MMCs [17] [18] [19].

A notable development during the year 2000 has happened in the field of Nano composites. Nano particle reinforced metal matrix composites came to be heavily researched around the world. Carbon nano tubes were extensively used for incorporating in almost all types of metal matrices. The fabrication technique along with heat treatment methods of nano composites were also discussed [20] [21] [22]. During this period, the investigators focused their research on the fabrication of nano metal matrix composites. This was due to the fact that MMC had firmly made their mark in various applications which are now called for mass production of these materials. Later the researchers tried to evolve ways to weld aluminum and titanium matrix composites via friction stir welding in particular that attracted numerous research interest. Many innovative methods such as spark plasma sintering of titanium matrix composites, drilling of SiC particle reinforced aluminum matrix composites, milling of magnesium matrix composites came into be existence [23] [24]. Squeeze casting technique that evolved as a proven fabrication technique in the past decade was successfully adopted by the engineers to produce aluminum matrix composites reinforced by discontinuous phase [25]. Investigators around the world have also worked mainly with aluminum, titanium-nickel, and nickel-Molybdenum and stainless steel matrices [26]. This period also witnessed the research on copper and magnesium as matrix materials. Later alloys gained a lot of attention and experiments were undertaken to alloy magnesium with aluminum and titanium for the matrix material [27] [28]. Hybrid composites, have recently became the most researched materials. Another point of interest proved to be in the field of fiber metal laminates. Incorporation of sandwich panels and metallic foams in various matrices was also studied during this period. Aluminum matrices reinforced with ceramic foams (mainly silicon carbide foam), while aluminum foam was used to reinforce a sandwich panel. The latter half of this decade belonged to the research on aluminum and magnesium matrix composites [29] [30]. A healthy research with this material is due to the fact that magnesium matrix composites have very low density along with excellent mechanical properties. Due to this fact, the aluminum matrix composites find their extensive use in structural, automotive and aerospace applications [31] [32] [33] [34] [35].

In the 21st century, research is still going on to develop the next generation MMCs by reinforcing with rare earth ceramic particulates such as beryl, neodymium, yttrium, cerium etc. as reinforcements in aluminum alloys composites. Rare earth elements such as yttrium, cerium and beryl have been used as additives in the preparation of advanced ceramic materials. Addition of these elements have found resulted in noticeable enhancement in mechanical, physical,

wettability and wear resistance properties of MMCs. In spite of popularity of the usage of rare earth materials as reinforcement in MMCs, no of research work is reported with regard to beryl ceramic reinforced in chilled aluminum alloys [36]-[41].

3. Experimental Procedure

3.1. Matrix Material (LM-13 Al Alloy) and the Reinforcement (Beryl)

Commercial grade aluminum alloy (LM-13) was selected as the matrix material which is of great importance in automotive and aerospace sector. LM-13 aluminum alloy is known for its excellent mechanical properties due to the presence of a good percentage of silicon along with the right amount of magnesium and manganese that has made LM-13 the most suitable material for the matrix. Table 1 and Table 2 below show the chemical composition and properties of LM-13 aluminum alloy used in the present research.

Beryl is a mineral composed mainly of beryllium aluminum cyclosilicate with the chemical formula $Be_3Al_2Si_6O_{18}$. Well-known varieties of beryl include emerald and aquamarine a naturally occurring hexagonal crystal available in different sizes and colors (Table 3, Table 4).

3.2. Molding and Composite Making.

Molds were prepared according to AFS standards (5% bentonite as binder and 5% moisture with special additives) along with standard runners and risers. End chills were inserted in the mold in the desired location and finally molds were dried in the air furnace, in the present investigation.

Copper end chills of different thickness (10, 15, 20 and 25 mm) were used. For each chill thickness, the reinforcement addition was varied from 3 to 12 wt.% in steps of 3 wt.%. The reason for using copper chills of different thickness is to vary the volumetric heat capacity (VHC) of the chill which in turn varies the heat extraction capacity and hence variations in microstructure and mechanical properties. Note that copper is selected as the chill material because of its good thermal conductivity, availability, ease of fabrication and the cost.

Matrix material (LM-13) was melted and super-heated to 700˚C to which preheated reinforcement (up to 400˚C) was introduced evenly into the molten alloy by means of special attachment and stirred well by a stirrer at a speed of 300 rpm to create vortex for uniform and thorough mixing of the reinforcement in the matrix and at the end of stirring the degassing tablet was added in to the melt. Finally the reinforcement treated melt was poured in to the mold cavity containing the end chill and allowed to solidify. For testing purpose, specimens were selected only from the chill end. Note that all the test samples before mechanical testing were subject to aging heat treatment process to remove residual stresses. Figure 1 shows the dimension of the mold cavity and the end chill set in position.

Table 1. Chemical composition of the matrix alloy (LM 13).

Elements	Zn	Mg	Si	Ni	Fe	Mn	Al
by wt. %	0.5	1.0	12	2.0	0.5	1.0	Bal

Table 2. Properties of LM-13 aluminum alloy.

Property	UTS (MPa)	Hardness (HV)	Melting point O˚C	Density (gm/cc)	Structure
	155	125	698	2.7	FCC

Table 3. Chemical composition of beryl particle.

Composition	SiO_2	Al_2O_3	BeO	Fe_2O_3	CaO	MgO	Na_2O	K_2O	MnO
by wt. %	65.40	19.08	12.30	0.80	1.34	0.48	0.55	0.004	0.05

Table 4. Properties of Beryl.

Density g/cc	Hardness (VHN kg/mm^2)	Melting point (˚C)	Type of structure	Color
2.6 - 2.8	890	2500-2700	Hexagonal	Emerald green/color less

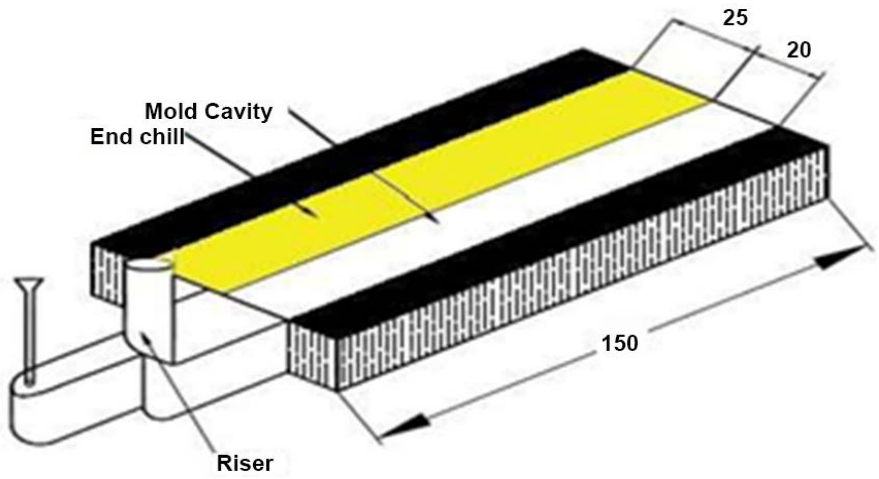

Figure 1. AFS standard mold cavity along with the end chill in position.

3.3. Testing

The microstructural examination was performed on the neatly polished specimens using Nikon Microscope LV150 with CEMEX image analyzer according to ASTME 3 standards. Standard metallurgical procedure was followed for the specimen preparation and all the specimens were etched with Keller's reagent before testing. XRD analysis was also carried out for copper chilled composites to confirm the chemical composition of reinforcement, matrix alloy and formation of any other secondary phases. Tensile strength test was performed on a tensometer specimen using Instron testing machine according to ASTM-E 8M standard. Hardness tests (HV) of all the heat treated specimens were performed on

the polished specimens used for microstructural studies using a digital Vickers micro-hardness tester (model-MMT X7A) under a load of 100 gm for 15 seconds. Wear studies were carried out by Ducom make computerized pin on disc wear testing machine according to ASTM G99-17 standard.

Note that all the above tests were conducted on the chilled composites developed and each test result is obtained from an average of three samples drawn out from the same location near the chill end.

4. Results and Discussion

4.1. Microstructure of the Chilled Composite

Figure 2 shows the XRD pattern of only beryl reinforcement which confirms the presence of phases like BeO and Al_2O_3 which are the main constituents forming the chemical composition of beryl.

Figure 3 shows the XRD spectrum of the composite containing these particles confirming the presence of Al, SiO_2 and BeO phases in LM-13-beryl particulate composite. It can be seen that only very few peaks are observed in this spectra suggesting the amount of beryl particles are few as compared with other constituents. This XRD analysis test report of the composite developed (25 mm thick copper chilled MMC with 9 wt.% reinforcement) indicating the presence of constituents of the matrix alloy as well as the reinforcement indicates the reinforcement is thoroughly mixed in the composite.

Microstructure of the composite developed in the present research primarily depends on the rate of chilling as well as on the reinforcement content that influences solidification. As usual it is observed from microstructural studies of the un-reinforced and un-chilled matrix alloy (microstructure not shown) that the

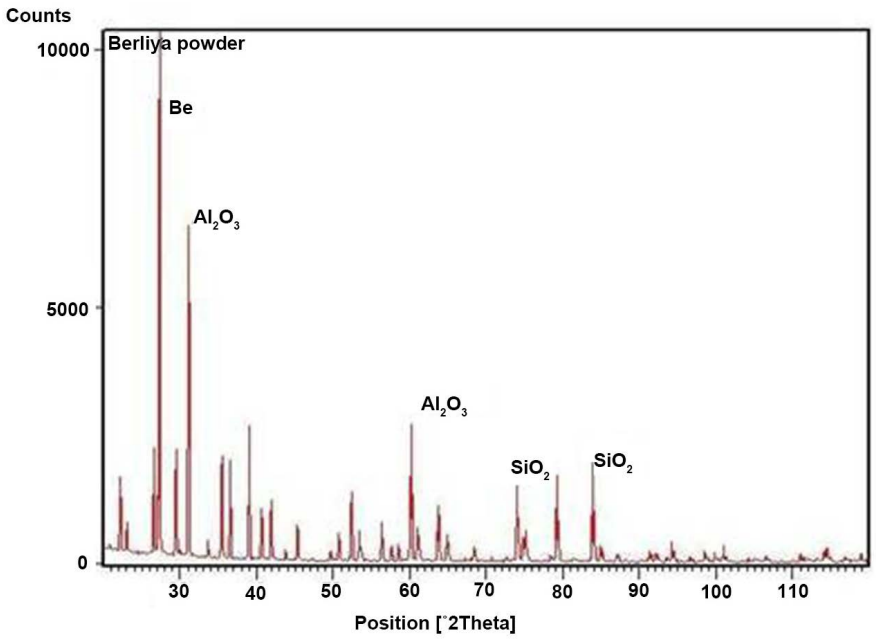

Figure 2. XRD pattern Beryl particle.

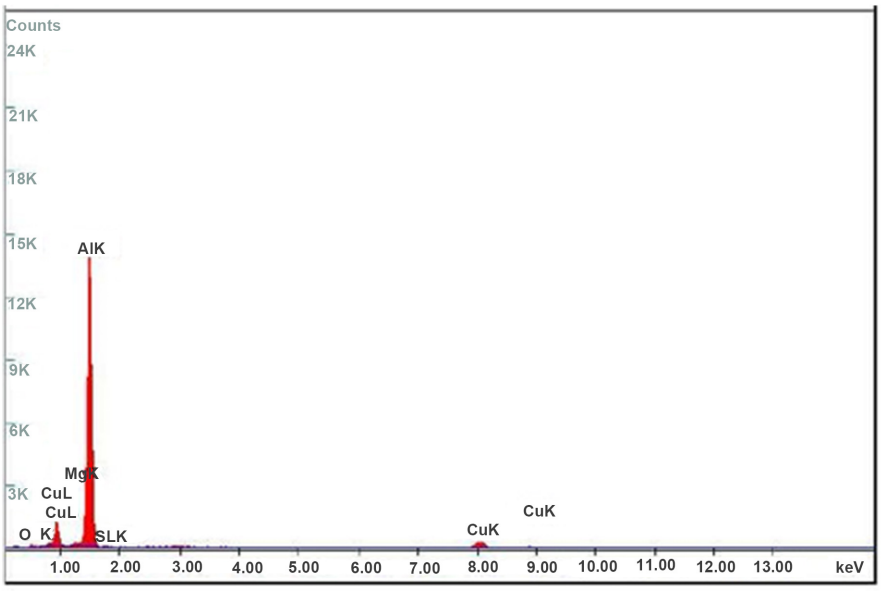

Figure 3. XRD spectrum of the composite containing Beryl particles.

presence of un-fragmented dendritic structures shows the presence of equiaxed grain structures. The microstructure also reveal the growth of α aluminum dendritic network structure surrounded by α-$CuAl_2$ which is formed due to under-cooling of the casting during solidification, with less impurities present. This is because, it is well known that aluminum being a long freezing metal and it is difficult feed during solidification. Feeding during solidification is enhanced by incorporating the end chills which in turn also makes the casting sound. Hence the microstructure of chilled MMCs reveals fine grain structure without any micro-porosity.

Figures 4-7 illustrate the photo-micrographs taken at 500× magnification for etched specimens with varied reinforcement content (3, 6, 9 and 12 wt.%) cast using the copper end chill of 25 mm thickness. It is observed from the microstructure that the grain fineness increases as the chill thickness increases and fine grain structure and good mechanical properties were obtained for chilled MMCs cast using 25 mm thickness because if its high VHC. But at higher percent of addition of reinforcement (beyond 12 wt.%), it is observed that there is segregation/clustering of the reinforcement (microstructure not shown) especially near the grain boundaries. It can be seen that the particles are evenly distributed at the inter dendritic regions of 3, 6 and 9 wt.% reinforcement content chilled composite whereas for 12 wt.% reinforcement composite, micrographs show fewer particles at the inter-dendritic region. This may be due to the increase in density difference ensued at higher concentration of reinforcement within the matrix resulting in settling down and/or clustering of the reinforcement. Hence, adding reinforcement content beyond 12 wt.% do not serve the purpose. Therefore all further focus of the discussions will be based on chilled MMCs with 12 wt.% reinforcement cast using copper chill of thickness 25 mm.

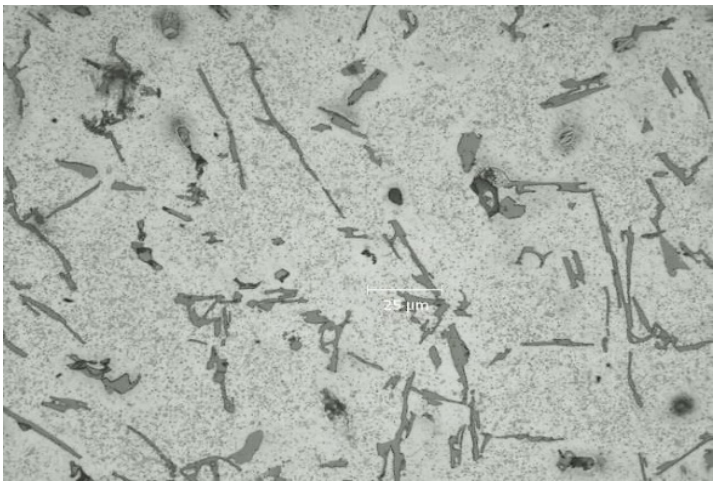

Figure 4. Microstructure of 3 wt.% composite cast using copper chill of 25 thickness.

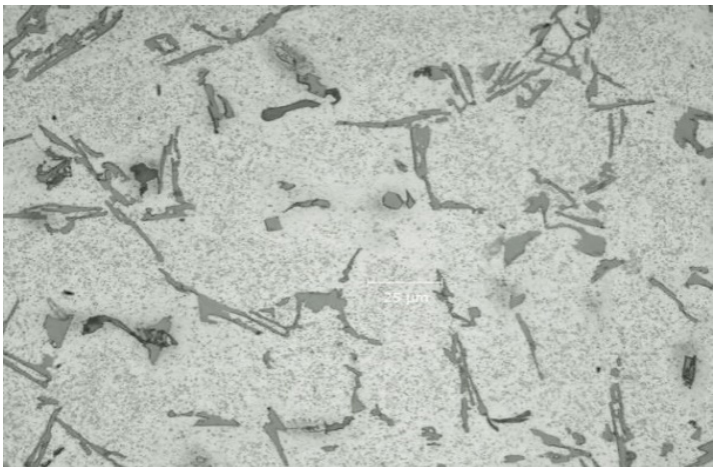

Figure 5. Microstructure of 6 wt.% composite cast using copper chill of 25 mm thickness.

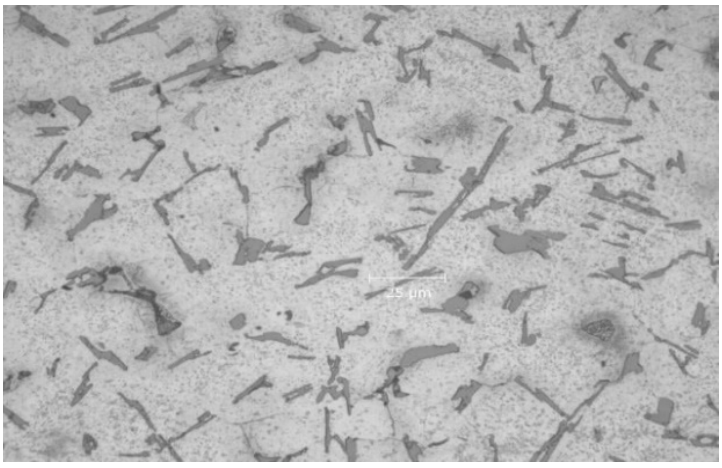

Figure 6. Microstructure of 9 wt.% composite cast using copper chill of 25 thickness.

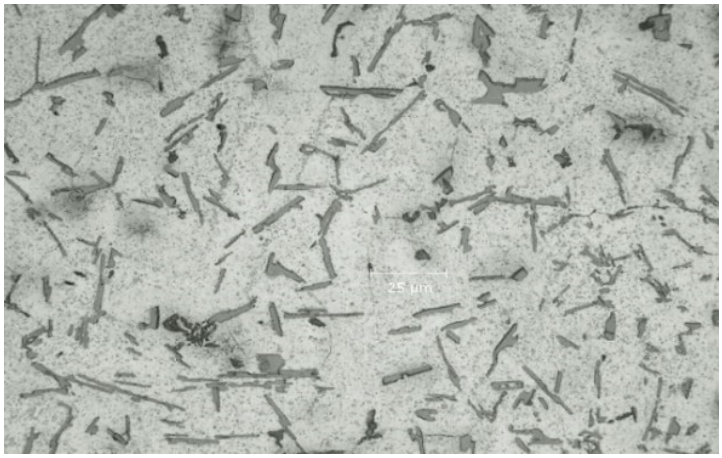

Figure 7. Microstructure of 12 wt.% composite cast using copper chill of 25 thickness.

Figures 4-7 are the microstructure of different composites cast using copper chill of 25 mm thickness (Magnification 500×).

The photo micrographs reveal the fact that there is an almost linear relationship between the uniform distribution of the reinforcement within the matrix alloy and the weight percent of reinforcement present in the matrix. Microstructure of the chilled MMCs is also discussed in terms of distribution of reinforcement and matrix reinforcement interfacial bonding. It is observed from the microstructure that for the chilled MMCs containing lower amount of reinforcement (3 and 6 wt.%) revealed that there is no formation of clusters or segregation near the grain boundary but with good matrix and reinforcement integrity. This may be due to gravity of the reinforcement particles associated with judicious selection of the stirring mechanism (vortex route) and good wettability of the pre-heated reinforcement by the matrix melt.

It is observed from the microstructure that the MMC fabricated using copper chill of 25 mm thick (having highest VHC) has a very fine grained structure because of the steep temperature gradient setup during solidification. This has made proper flow of liquid metal in to the inter-dendritic spaces making the bond strong without any porosity. Examination of the photo micrographs indicate that the microstructure consisting of fine eutectic silicon (dark gray) dispersed within the inter-dendritic region (light gray matrix) and fine precipitates of alloying elements in the matrix of aluminum solid solution. It is also observed that the fine grain structure is due to grain refinement and it was extremely good in the case of copper chilled MMCs cast with of 25 mm thickness, whereas coarse grain structure was observed in the case of MMCs cast with copper chills of lower thickness. However the grain refinement and reinforcement distribution is primarily attributed to the capacity of the reinforcement particulate to nucleate from matrix aluminum alloy during the directional solidification under the influence of chills that restricted the growth of aluminum grains because of the presence of finer reinforcement.

Note that he rate of solidification has a direct influence on the size and structure of the dendrite arm spacing. Steeper and higher cooling rates (effect of chilling) result in smaller dendritic arm spacing than the reinforcement size. This drastically reduces the movement of the reinforcement within the matrix resulting in a fewer segregation during solidification. Hence, it is always desirable to have a dendritic arm spacing of either less than or equal to the particle size to ensure a uniform distribution of the reinforcement within the matrix. The rate of solidification in the present work is directly related to the VHC of the chill used. Therefore a smaller dendritic arm spacing is obtained in composites cast with copper end chill of 25 mm thickness which is having a greater VHC as compared to other copper end chills used in the present research. It is observed from the microstructure that the reinforcing particles during solidification are generally trapped between the dendrites. This trapping is usually more pronounced at the hinder side of the dendritic tip and for the first few secondary branches. The reinforcement that is placed within the secondary branches tends to remain trapped between the branches as the dendritic growth propagates. The particles that settle at the hinder side of the tip appear at the dendritic base after the complete solidification process.

4.2. Mechanical Properties

4.2.1. Ultimate Tensile Strength (UTS) of the Chilled Composite

Recently, metal matrix composites are being widely used as structural, automobile and aerospace material owing to their increased strength coupled with an extremely good strength-to-weight ratio. This is primarily due to the fact that the composites transfer the applied load onto the harder reinforcements via a soft and ductile matrix metal. In order to realize this, an imperative chilling of composites was introduced in the present research to ensure a strong interfacial bonding between the different phases making up the composite dense, sound and free from micro-porosity. It is well known that the difference between co-efficient of thermal expansion of matrix and reinforcement leads to increase in dislocation density. This increase in dislocations will be inhibited near the grain boundaries, requiring higher energy (*i.e.* loading) to keep their movement across the grains. This is also one the reason for increase in UTS up to 9 wt.% addition of the reinforcement and addition of the particles beyond 9 wt.% decreases the strength and this decrease can be attributed to agglomeration and segregation of the particles towards the eutectic phase. The agglomerated particles would present a weaker zone in the structure, which may act as a crack initiator in the specimen and hence lowers the strength.

Figure 8 shows the effect of reinforcement content on Ultimate Tensile strength (UTS) for various MMCs cast using different types of chills. It is observed that UTS is again maximum for the chilled composite cast using copper chill of thickness 25 mm (maxm. VHC) and least for the copper chill of 10 mm thickness (low VHC). Further, it may be observed from **Figure 7** that, the effect of increasing the thickness of the chill (to increases the VHC) increases UTS. It

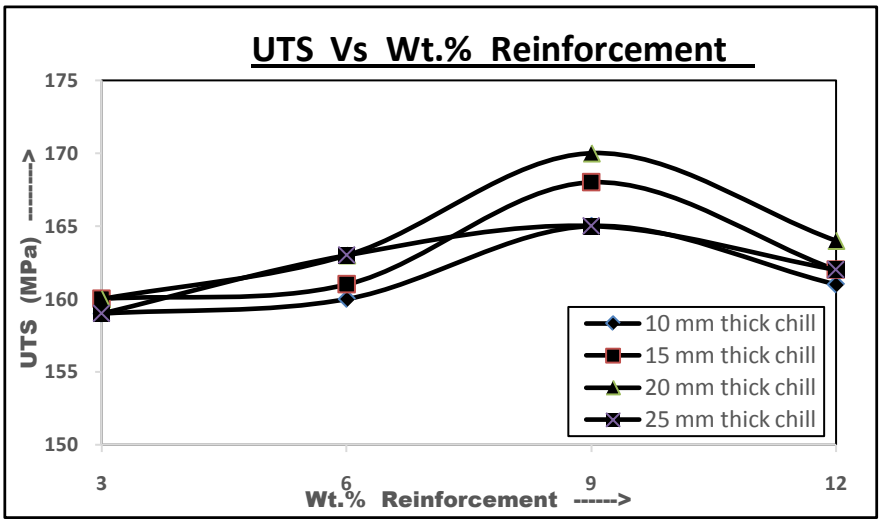

Figure 8. Plot of UTS vs. wt.% reinforcement for MMCs cast using different chills.

is also observed from the microstructure as well from the strength test results that, increase in the reinforcement content increases UTS up to 9 wt.% and beyond which it decreases due to even distribution of the reinforcement and cluster formation. These clusters act as stress risers concentrated at that location fails to transfer the load and hence the strength falls. In most cases, ceramic reinforced MMCs have superior mechanical properties compared to the un-reinforced matrix alloy because these MMCs have high dislocation densities due to dislocation generation as a result of differences in coefficient of thermal expansion [42]. As in this study however, with the incorporation of beryl particulate reinforcement has a major effect in improving mechanical properties. Standard results reveal that the UTS of the matrix aluminum alloy (LM-13) used in the present research is around 155 N/mm^2. Whereas in the present research, the UTS obtained for aluminum alloy (LM-13) reinforced with beryl particulate cast using different chills of different VHCs ranges from 160 to 172 N/mm^2. It is observed that the strength of chilled MMC was found to increase by 9.88% as compared against the matrix alloy. The increase in UTS suggests that beryl particulate as reinforcement and chilling has an effect on the UTS. However the past research indicates that the strength of the composite depends on the reinforcement, interfacial bond between the matrix and the reinforcement, distribution of the particles as well as on the size of the particles [43]. But in the present investigation in addition to all the above parameters, sound casting with fine grain structure was obtained due to chilling, vortex method of stirring and preheating of the reinforcement has played a vital role in further increasing the UTS. Microstructural studies reveal that chilled MMCs are denser without any micro-porosity UTS. is also the reason for the increase in From the results of the mechanical characterization of chilled Al-alloy (LM-13) and beryl MMCs, one can conclude that strength depends on reinforcement content and chilling effect.

In order to confirm the above discussions, fractographic analysis of the spe-

cimens failed in strength test was under taken using SEM. Figure 9 and Figure 10 show the SEM fractographs (at 100× and 100 μm) of the fractured specimens containing 9 wt.% reinforcement MMC cast using the copper chill of 25 mm thickness as well as the un-chilled bare LM-13 aluminum ally. It is observed that for the bare aluminum matrix alloy (LM-13), fracture was in pure ductile mode containing large amount of dimples (Figure 10) and failure is due to propagation of the cracks near the grain boundary. Here again the size of the dimples present in the fractured surface depends on the silicon content of the alloy. For copper chilled (25 mm thickness) MMC with reinforcement content of 9 wt.%, the composite has become little brittle and the SEM of the fractured sample (Figure 9) showed mixed mode of fracture. At higher percent of addition of reinforcement (beyond 9 wt %, fig not shown), cluster formation of the reinforcement was observed in the microstructure with poor interfacial bonding that has caused the trans-granular type of brittle fracture. Therefore the size of the dimples in the fracture surface exhibits a direct proportional relationship with strength and ductility of the MMC *i.e.*, finer the dimple size increases the strength and ductility of the MMCs developed.

It is well known and documented by several researchers that ductility of discontinuous reinforced MMC's decreases with an increase in reinforcement content. Hence the percent elongation is always inversely proportional to UTS. This is one of the reasons that reinforcement has an effect only up to certain amount of addition.

4.2.2. Hardness of Chilled Composite

In comparison to ferrous materials, aluminum alloy is soft, ductile and possesses lower hardness. Hence, it becomes extremely difficult to use aluminum and its alloys in abrasive/wear environments. To overcome this difficulty, aluminum alloys are reinforced with hard ceramic reinforcements so that the composite is rendered as wear resistant. In the current research, hard beryl particulates are embedded in softer LM-13 aluminum alloy to make the composite harder than the matrix material.

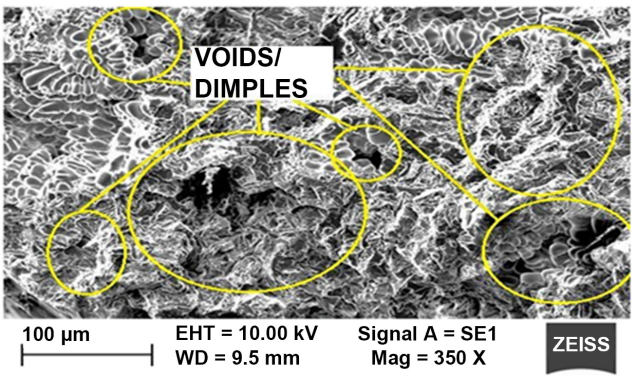

Figure 9. SEM fractograph of 9 wt.% composite cast using copper chill 25 mm thickness (100× and 100 of μm).

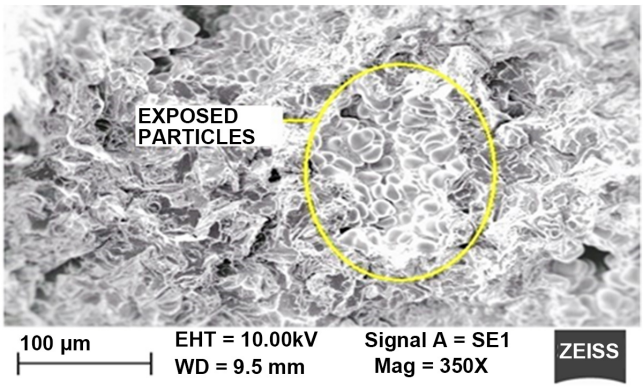

Figure 10. SEM fractograph of LM-13 Al alloy (100× and 100 µm).

Hardness tests were conducted only after subjecting the test samples to aging heat treatment process. From the past research of the present author, if all other factors are kept constant, the aging rate of a composite is generally faster than that of the matrix alloy [44]. After solution treatment, optimum aging conditions can be determined by observing the hardness of the MMCs cast using chills for different aging durations. It is known that the optimum aging conditions are strongly dependent upon the amount of reinforcement present [45]. It can be seen that for each MMC, as the aging time increases, the hardness of the MMCs increases to a peak value and then drops again. As reinforcement content is increased, there is a tendency for the peak aging time to be reduced because reinforcement provides more nucleation sites for precipitation. As expected, for any fixed aging temperature and duration, increasing the reinforcement content causes the hardness of the MMC to increase since reinforcement particulates are so much harder than the aluminum alloy matrix [46].

Figure 11 shows hardness of chilled MMCs cast using chills of different thickness. The results of micro hardness test (HV) conducted on chilled MMCs samples revealed an increasing trend in matrix hardness with an increase in reinforcement content (up to 12 wt.%). Results of hardness measurements also revealed that the thickness of chill has an effect on hardness of the composite. This significant increase in the hardness can be attributed primarily to presence of harder ceramic particulates in the ductile matrix that has higher constraint to the localized deformation during indentation because of reduced grain size due to chilling. In ceramic-reinforced composites, there is generally a big difference between the mechanical properties of the reinforcement and those of the matrix. These results in incoherence and a high density of dislocations near the interface between the reinforcement and the matrix [47]. Precipitation reactions are accelerated because of incoherence and the high density of dislocations act as heterogeneous nucleation sites for precipitation [48].

It is observed from the results of the hardness test that hardness of the composite increases linearly (up to 12 wt.% addition) as the reinforcement increases and maximum harness was observed in the case of composite cast using the

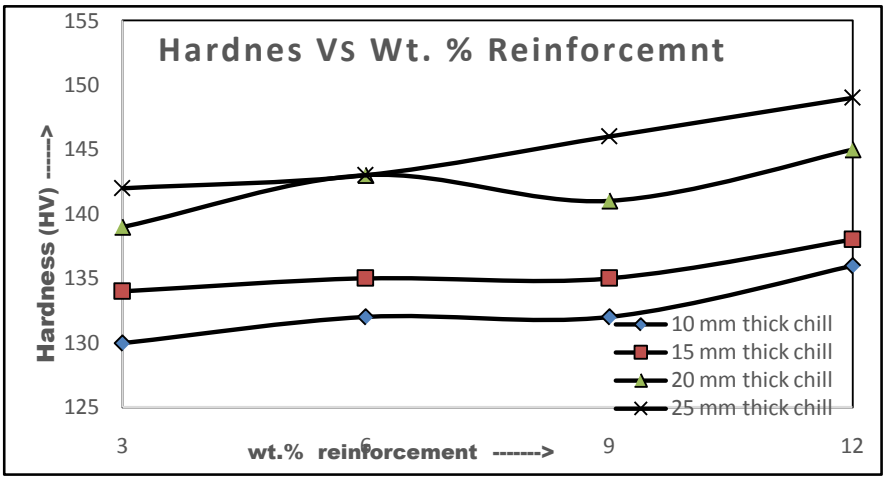

Figure 11. Plot of hardness vs. wt.% reinforcement for MMCs cast using different chills.

copper chill of 25 mm thick. This increase in hardness in turn increases the wear resistance of the composite developed that suits automotive application. It is observed from Figure 11 that beyond 12 wt.% addition, the hardness decreases because of cluster formation and segregation of the reinforcement as evident from the microstructural studies. VHC of the chill has an effect on the hardness of the composites developed since chilling refines the grains in reducing the grain size that again offers resistance to indentation. It is observed that of all the copper chills, copper chilled composites cast with 25 mm thickness have attained the maximum hardness because of its high heat extraction capacity. It is also observed that maximum hardness was observed for all the composites developed were near the chill end and it decreases towards the riser end. This again shows that chilling has an effect on the hardness.

Standard results reveal that the hardness of the matrix aluminum alloy (LM-13) used in the present research is around 125 HV. Whereas in the present research, the hardness obtained for aluminum alloy (LM-13) reinforced with beryl particulate cast using different chills of different VHCs ranges from 130 HV to 150 HV. It is observed that that hardness of chilled MMC is found to be increased by 16.66% as compared against the matrix alloy. The increase in hardness suggests that beryl particulate as reinforcement and chilling has strong effect on the hardness.

4.3. Tribological Behavior of the Composite

4.3.1. Friction and Wear

Figures 12(a)-(c) show the variation in weight loss of the composite (containing 9 wt.% reinforcement cast using chills of different thickness) as a function of sliding distance tested at loads 10, 20 and 30 N respectively. At the lowest load (10 N) in mild wear regime a high coefficient of friction was always found for all the composites tested. At higher loads (30 N), the composite containing 12 wt.% reinforcement cast using 10 mm tick chill exhibited severe wear with a better

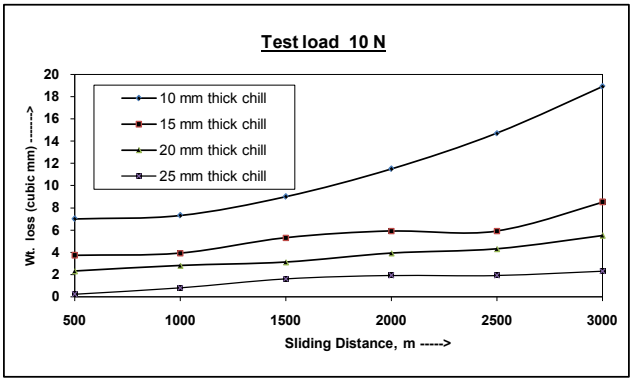

(a) Low Load

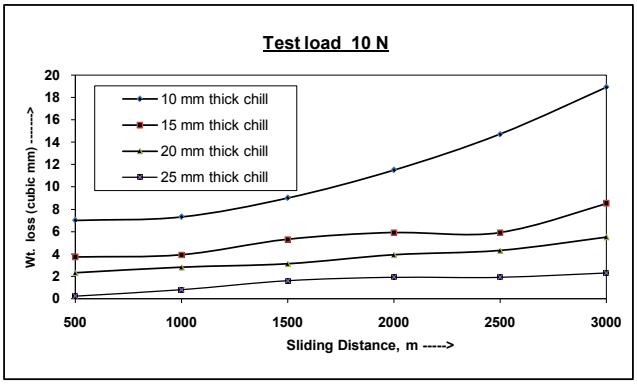

(b) Medium Load

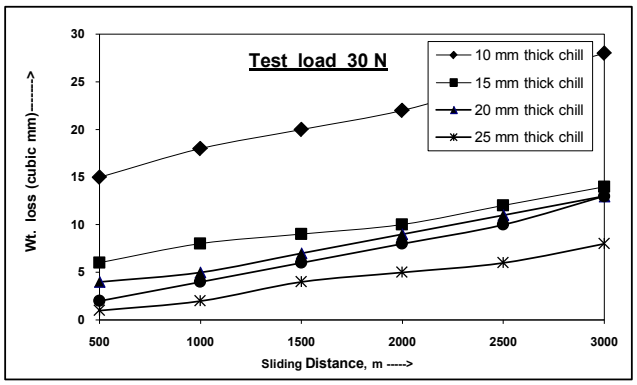

(c) High Load

Figure 12. Plot of wt. loss vs. sliding distance of 9 wt.% reinforcement composite cast using chills of different thickness tested at different loads.

wear resistance as compared with the matrix alloy. Chilled composites cast using chills of lower VHC, tested at all loads underwent large weight loss during the early stages of the test. After sliding for some distance, the weight loss increased approximately linear with sliding distance. The sliding distance for transition from severe to mild wear could be identified by two factors: Firstly, by abrupt and steep reduction in the frictional force, and secondly, by change in the magnitude of displacement of pin specimen [49]. Based on these measurements, the wear curves are characterized by two distinct lines of different slopes, which correspond to severe and mild wear conditions. Composite containing 12 wt.% reinforcement cast with 25 mm thick chill showed steady state mild wear from the beginning of the test. At no point during the test the severe wear was noticed. It was also observed that, the sliding distance and weight loss during the severe wear regime decreases with an increase the chilling thickness. In the case composites cast with 25 mm copper chill with 15 wt.% reinforcement (fig. not shown), severe wear did not occur at all. These wear rates in the severe wear regime was calculated by dividing the weight loss by the sliding distance of severe wear. In the severe wear regime, wear rates of composites decrease with increasing the chilling thickness and hence the rate of chilling. The transition to lower wear rates (mild wear regime) is accelerated with increasing in heat capacity of

the chill. It is obvious that chilling effectively prevents the time/distance required for transition from severe to mild wear.

The mean steady state values of the coefficient of friction (μ) as a function of sliding speed tested at loads 10, 20 and 30 N are reported in **Figures 13(a)-(c)** respectively for chilled composites cast using chills of different thickness. At the lowest applied load of 10 N and at the lowest sliding speed of 0.3 m/sec a very high coefficient of friction about 1.0 was measured for the un-chilled composite in the mild wear regime and for the chilled composites it was reduced to around 0.76 as shown in **Figure 13(a)**. At intermediate sliding speed (1.2 m/sec) the coefficient of friction decreases in the mild wear regime and finally at higher sliding speeds (1.8 m/sec) all the steels displayed the same frictional behavior with coefficient of friction value around 0.55. With an applied load of 20 N and at the lowest sliding speed a high coefficient of friction of 0.92 was measured for the un chilled composite in the mild wear regime, whereas for the chilled composite it was decreased to 0.7 - 0.87 as shown in **Figure 13(a)**. At the highest applied load of 30 N and at the lowest sliding speed a high coefficient of friction of 0.9 was measured for the un-chilled steel which displayed a mild wear regime, whereas the chilled composite at the same sliding speed was decreased down to 0.6 - 0.8 as shown in **Figure 13(c)**. At intermediate sliding speed the trend is that, a high coefficient of friction was measured in the mild wear regime and decrease to lower values of 0.35 - 0.5. At the highest sliding speed all the chilled composite displayed the same frictional behavior with a lower value of coefficient of friction around 0.55 independently from the applied load the wear regime.

4.3.2. Effect of Chilling on Severe Wear

Effect of chilling changes the microstructure (dense and fine grained structure) of the composite that affects wear behavior. The observation made using the optical microscope (**Figure 14**) clearly reveals beryl reinforcement contained in LM-13 matrix alloy is accompanied by the deformation and hence the micro cracks. The depths of the deformation zone where the beryl was deformed, was measured in order to obtain the depth of the plough region. These depths were found to be 42 μm for un-chilled composite and 19 μm for chilled composite containing 12 wt.% reinforcement cast using chill of 25 mm thick. It was also observed that the depth of the deformation zone decreases with increasing the VHC of the chill. Further, the cracks propagate in the subsurface as a result of adhesion and deformation. In the beginning of the wear test, the plastic flow of the composite containing 12 wt.% reinforcement cast using chill of 25 mm thickness, was appreciable and thus causes severe wear. But in the case of chilled MMCs (containing 12 wt.%), the formation of a hard surface consisting of beryl particles in LM-13 matrix alloy helps in preventing adhesion. As a result, transition from severe wear to mild wear occurs and concomitantly the wear rate is reduced as a result of removal of wear debris as a lower rate. In composites cast using 25 mm thick copper chill, containing 12 wt.% reinforcement, the

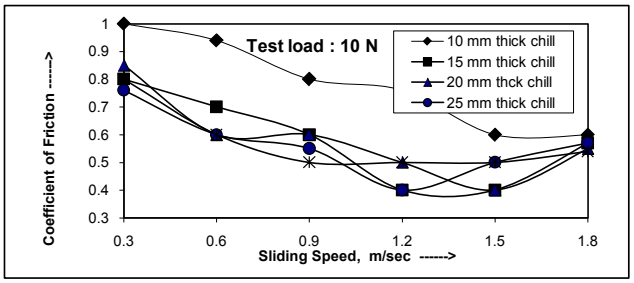

(a) Low Load

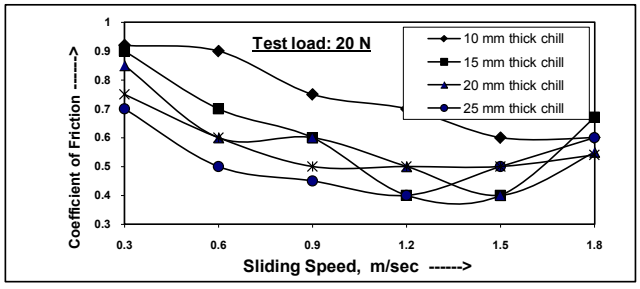

(b) Medium Load

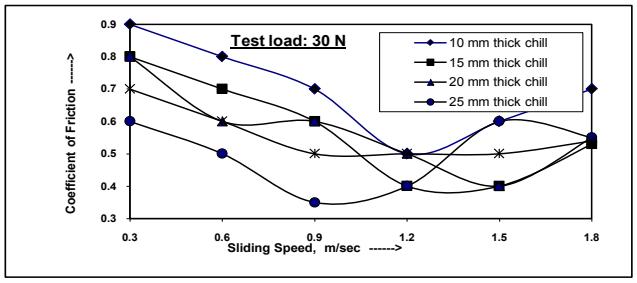

(c) High Load

Figure 13. Plot of coefficient of friction vs. sliding distance for composite (9 wt.% reinforcement) cast using chills of different thickness tested at different loads.

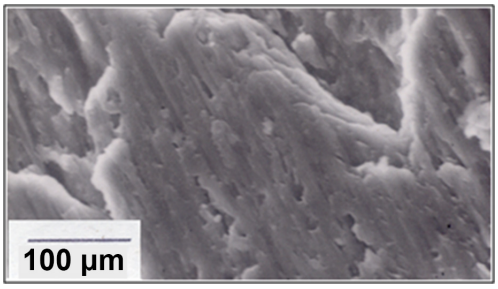

Figure 14. SEM photograph showing the cross section parallel to the sliding direction for LM-13 Al matrix alloy in the severe wear regime.

deformation was prevented because of the beneficial effects of the grain size and strong bonding. Therefore it is considered that severe wear caused by the adhesion disappears with increasing the chilling rate.

4.3.3. Effect Chilling on Mild Wear

Figures 15(a)-(d) show SEM photograph of the worn surfaces of different chilled composites cast using chill of 25 mm thickness in the mild wear regime. It is observed that for the composite cast with 3 wt.% reinforcement, the worn surface was completely smooth, flat and contained wear tracks in the direction of sliding. In addition, the signature of plastic flow was not at all observed on the subsurface. In contrast, the composite containing 6 and 9 wt.% cast using copper chill of 25 mm thick, the worn surface of composite was found to be rough containing the debris. Microscopic examination of its subsurface shows fragmentation and their uniform dispersion on the entire worn surface and, as a

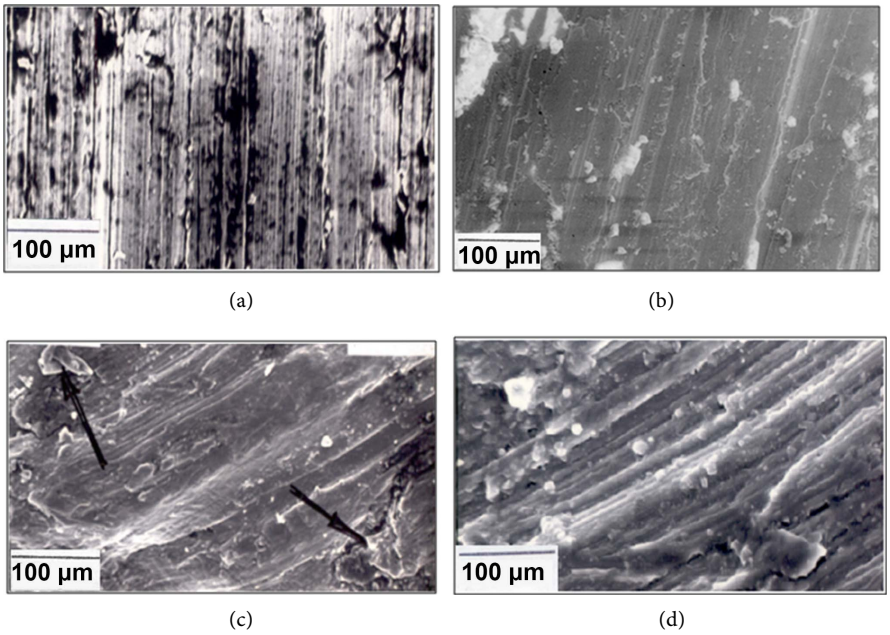

Figure 15. SEM photomicrograph of worn surface of various composites cast using copper chill of 25 mm thickness in the mild wear regime (100×, 100 µm). (a) 3 wt.% composite; (b) 6 wt.% composite; (c) 9 wt.% composite; (d) 12 wt.% composite.

result, plastic flow was very limited. Further, in the case of sub the surface of composite containing 12 wt.% reinforcement cast using 25 mm thick chill was found to be very rough with a characteristic brittle fracture. The subsurface region consisted of fragments of crushed beryl (indicated by an arrow in **Figure 15(d)**). This shows that mild wear is dominated in composites cast using copper and chill of 25 mm thick. A very thin tribo-induced layer was formed on the entire surface and, in addition some particle was projected onto the surface. The lengths of the crushed carbides were measured for more than 10 fragments on the several cross sectional micrographs. The mean length was found to be 6 µm (ranging from 3.5 to 8 µm) for 9 wt. reinforced composites cast using 25 mm thick chills. From these detailed observations, it becomes obvious that the reinforcement present were crushed into small fragments and a thin layer is formed on the smooth surface containing wear tracks confirming abrasive wear in the mild wear regime.

4.3.4. Wear Mechanism Model

Wear mechanism of the present investigation is suggested by two modes. Mode-1 refers to adhesive wear (severe wear) and is predominant in the composite containing 3 wt.% reinforcement and also in composites cast using lower chill thickness at higher loads. This type of wear disappears as the rate of chilling increases. On the other hand, Mode-2, which is essentially abrasive wear (mild wear) as result of embedded hard beryl particles in matrix alloy exposed on the worn surface and the loose fragments between two surfaces, dominates in composites containing 9 wt.% reinforcement cast using chill of high VHC (copper chill of 25 mm thickness).

SEM examination reveals that the worn surface of the chilled composite consists of both hardened and deformed layers. The structure of the hardened layer consists mainly of the fragmented reinforcement phase. The depth of this layer depends on the applied load and is in the vicinity of 10 to 25 μm. However, the depth of the hardened layer in the composite is markedly reduced by increasing the chilling rate. Moreover, the hardness value of the hardened layer in the chilled MMCs is considerably higher than that of the UN chilled composites. **Figure 16(a)** and **Figure 16(b)** show the wear mechanism of chilled composite in the mild wear conditions. Because of limited plastic deformation in the mild wear regime chilled MMCs, the micro structural studies reveal that, the fragmentation of the reinforcement appears as brittle fracture and in the case of composite containing 9 wt.% reinforcement, the plastic flow observed is due to deformation of the matrix alloy.

4.3.5. Relationship between Microstructure, Load and Wear

In the two body abrasion, the major portion of the load applied during testing is transferred to the specimen and the wear of the material took place under high stress condition [50] [51]. This is supported by the experimental results, as evident by the increase in transition load from severe to mild wear with the chilling rate [52]. These explanations are in line with earlier reports of Moustafa [53] that have shown an increase in the load for transition from mild to severe wear.

The hard beryl particles in chilled composites act as protuberances in the matrix alloy and bear the major portion of load and as a consequence, protect composite from wear. This leads to the reduction in wear rate of the chilled composite due to reinforcement of hard particles in the matrix alloy of the chilled composite. It is well known that the wear rate is significantly dependent on the applied load, microstructure and hardness of the material. The cutting efficiency of the disc particles increases with an increase in the applied load. As a result, more material is removed at higher loads and hence the wear rate increases with an applied load. The depth and width of cutting grooves also depends on the hardness of the material [54]. Since the hardness of the un-chilled

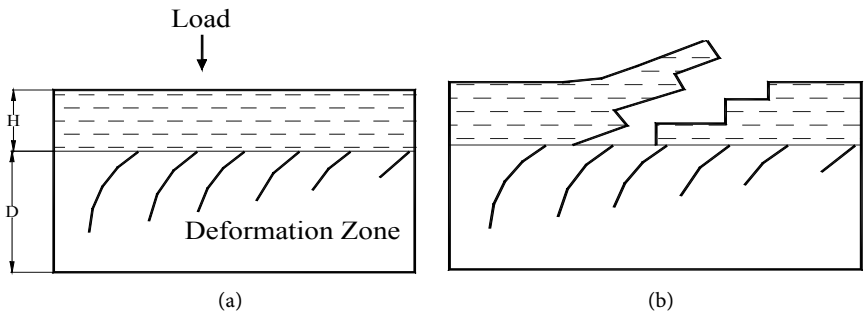

Figure 16. Schematic diagram showing (a) wear mechanism of 25 mm thick chilled composite containing 3 wt.% reinforcement indicating alignment and redistribution of beryl phase. In the deformation zone (D) leading to the formation of a hardened surface layer (H) and (b) Fragmentation of beryl particle under mild wear condition for composite containing 9 wt.% reinforcement cast using copper chill of 25 mm thickness.

composite is lower than that of the chilled composite and hence, the wear rate of chilled composite becomes lower than that of the un-chilled composite. Therefore, the chances of fracturing of beryl particles in the aluminum matrix are less in the case of chilled composites. This led to considerably higher wear resistance of the chilled composites even at a high load regime. As a result, the removal of a material vis-à-vis the wear rate of the material is governed by deformation parameters, microstructure and hardness. Thus by increasing the strength and hardness between the matrix and the reinforcement by the effect of chilling, the cutting efficiency of the hard disc particles is reduced.

4.3.6. Relationship between Hardness and Wear

It is well known that the wear rate of the material decreases with hardness irrespective of the applied load. SEM studies of the chilled composites tested at different loads reveal that, at lower load (10 N), the variation of wear rate with hardness was marginal, but at higher load (30 N) considerable wear with hardness was noted. At lower load, mainly cutting type wear takes place and the subsurface deformation is negligible [55]. The beryl particles remain intact within the matrix and protect the specimen surface more effectively. Thus, at lower load, the surface deformation behavior is negligible. At higher load, both cutting and ploughing mechanisms are operating and the subsurface deformation becomes considerably high. Because of subsurface deformation, transverse and longitudinal cracks are generated on the wear surface [56] [57]. The subsurface deformation is governed by the mechanical properties such as hardness, ductility and strength, which are again influenced by chilling, microstructure and distribution of hard beryl particles. These may cause considerable reduction in the wear rate with an increase in hardness and strength when tests are conducted at higher applied load. The sub surface deformation of the un-chilled composite may vary because of different matrix micro-structure and mechanical properties. In addition to the initial hardness of the chilled composite, after a few cycles of motion of the sample against the abrasive media, the hardness of the wear surface of different samples increases. Apart from this, since the beryl particles are very fine and they may have the tendency to break into small particles and spread over the wear surface thus protecting the matrix alloy from severe wear. **Figure 17** shows the photo micrograph of fragmented beryl particles in the subsurface region for 25 mm thick copper chilled 9 wt.% reinforced composite in severe wear regime. This includes higher hardness of the surface of the chilled samples than their bulk hardness during testing. This in turn results in a significantly lower wear rate in the chilled composites as compared as compared to the un-chilled and chilled composites at higher applied loads. The cracking and removal of flaky materials and work hardening of the subsurface take place simultaneously over the specimen surface. The overall wear rate of the material would depend on the cutting action and work hardening rate of the chilled composites may be higher and it increases with an increase in hardness. Apart from this, the possibility of fracture and fragmentation of beryl particles are low in chilled

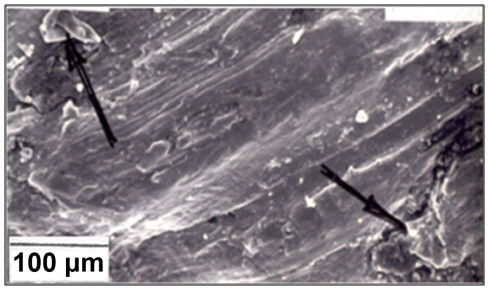

Figure 17. Photomicrograph of sub surface deformation of 9 wt.% reinforced composite cast using copper chill if 25 mm thickness showing deformed region depicting the fragmentation of beryl particles in the severe wear regime (100×, 100 μm).

composites because of the strong and hard reinforcement in the aluminum matrix as well as the effect of chilling. In fact the wear characteristics of the chilled composites are governed by the interaction of their chilling effect and hardness based on the reinforcement content present.

4.3.7. Worn Surfaces and Wear Debris

Wear debris generated during the mild wear regime was collected after the end of the wear test and examined under the microscope. SEM photographs of typical wear debris (marked inside the block) for different composites cast using chill of 25 mm thickness are shown in **Figures 18(a)-(d)**. The shape of the wear debris was mostly large and irregular in the case of the un-chilled composite and in case of chilled composites it was few and fine. From the observations of the worn surfaces and sub surfaces of chilled composites, it is clear that the generation and removal of wear debris is affected by the fragmentation of beryl particles. From SEM studies, it is recognized that beryl particles in wear debris were small and irregular in shape with sharp edges. Mean size of wear debris and the reinforcement fragments as a function of volume fraction are shown in **Figure 19**. It is observed from the results that the size of the wear debris decreases where as the reinforcement fragments remain more or less the same with increase in volume fraction of beryl particles. The reason for decrease in the size of the debris is as follows. Under compression, a brittle body is made smaller by crack propagation until a critical size and also due to non-attachment of it to the matrix of the material. But the particles below this size are deforming slightly rather than rapid cracking.

Under the mild wear conditions, it is observed in particular at the lowest load (10 N), the worn surfaces of the tested chilled composites were characterized by the presence of an oxide compact layer (about 20 μm) comprised of iron oxide. The presence of iron oxide is due to the abrasive action of the pin on the steel counter face [58]. Wear debris collected under conditions were in the form of very fine and rounded particles. XRD and EDX analyses showed that they were mainly comprised of SiO_2 and BeO particles. On the contrary, the micro structural observation reveals rough worn surfaces with grooves along the sliding

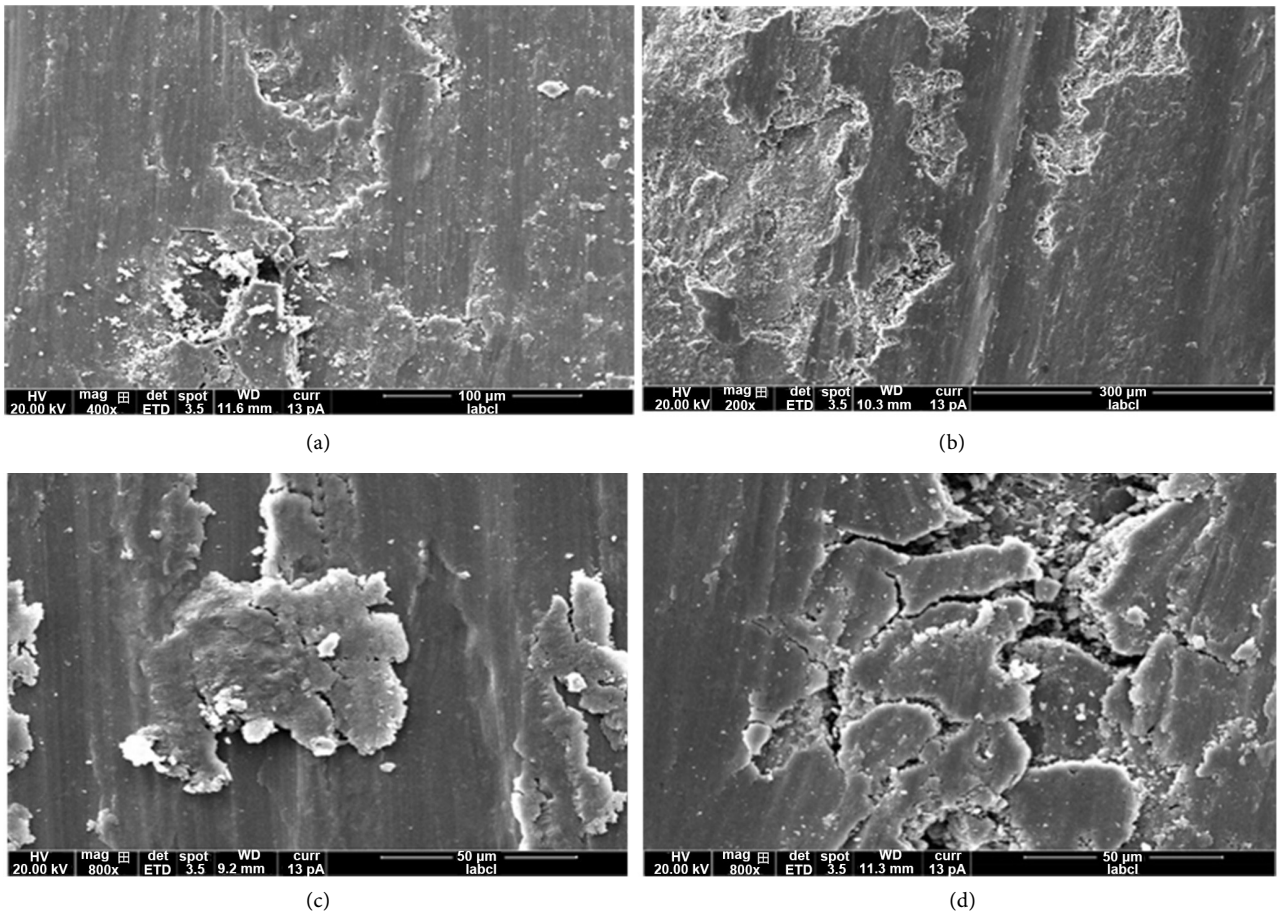

Figure 18. SEM photomicrograph showing wear debris of various composites cast using 25 mm thick chill in the mild wear regime (100×, 100 µm).

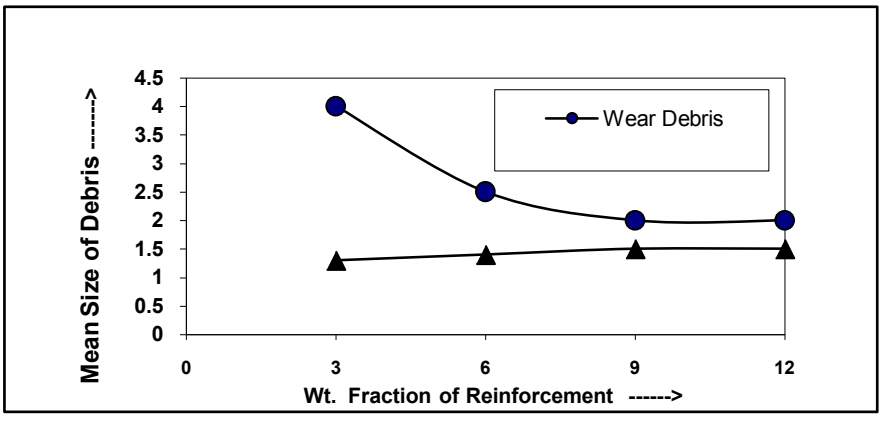

Figure 19. Plot showing the size of wear debris (in µm) and reinforcement fragments.

direction were observed in the severe wear regime. They were metallic in appearance, with some dark zones comprised of a mechanical mixed layer containing metallic iron, iron oxides and carbide fragments as confirmed by EDX and XRD analyses. According to Zhang *et al.* [59] in the mild wear regime, always observed at the lowest applied load (10 N), the worn surfaces of both the

un-chilled composite and the chilled composites were characterized by the presence of a protective iron-oxide rich transfer layer, suggesting that a material transfer process was active. Wear proceeded by spalling of this layer, producing fine and rounded oxide debris. The presence of beryl particles in chilled composite acts as a load bearing phase, limiting plastic flow and wear of the matrix. But at the same time plough into the Aluminum alloy abrasive wheel produces debris. These are continuously oxidized during sliding and transferred onto the counter facing sliding surfaces.

Longitudinal cross sections of the wear scars also analyzed by OM and SEM to characterize the subsurface deformation and to explain the superior wear resistance of the chilled composite with respect to the un-chilled composite. Micro-hardness tests on the longitudinal cross-sections of the same samples as a function of depth beneath the worn surfaces were carried out in order to evaluate the depth of the affected zone. In the case of 25 mm thick chilled composite with reinforcement content (9 wt.%), two layers were found. A first soft layer (about 110 μm) whose hardness was about 139 HV and a second hardened layer (about 30 μm) with a hardness about 143 HV. These results are in agreement with those obtained by Venkataraman *et al.* [60], who also observed a soft layer wherein the flow stress decreases with increasing shear strain, followed by a hardening layer, wherein the flow stress increases with increasing strain. The authors related the presence of the soft layer of the matrix alloy which transfer the load from the matrix ally and thus lower the strength of the chilled composites. Conversely, a slight strain-hardening in the shear zone (depth about 150 μm) just beneath the soft layer, it was found that the plastic deformation occurred at a higher depth, while the presence of the soft layer was not found.

5. Conclusions

In the present research, superior quality and sound Al-alloy (LM-13) reinforced with beryl particle chilled metal matrix composites was fabricated. Microstructural, mechanical and tribological characterization of the chilled composited developed reveals the following:

1) XRD analysis of the composite reveals that the reinforcement is thoroughly mixed along with the presence of all the compositions of the composite. XRD results also reveal the presence of beryl particles in the matrix alloy such as oxide phases of SiO_2 and BeO etc. that have dispersed uniformly throughout the composite.

2) Microstructural studies reveal that the reinforcement is uniformly distributed within the matrix with perfect bonding and fine grain structure (effect of chilling). Microstructure of the chilled composites is finer than that of the un-chilled steel composite with random orientation of beryl particles in matrix alloy.

3) The addition of beryl to Al matrix alloy has increased the tensile strength and hardness up to 9% wt. and 12 wt.% addition of the reinforcement. Strength and hardness of chilled MMC were found to be increased by 9.88% and 16.66%

respectively as compared against the matrix alloy. Increase in mechanical properties is attributed to the presence of the reinforcement content as well as the effect of chilling.

4) It is observed that because of the ceramic (beryl) reinforcement in aluminum alloy, the wear resistance of the chilled composite developed has increased with increase in reinforcement content. At lower load, chilled composites exhibited mild wear regime with high coefficient of friction and at higher loads they exhibited severe wear with better wear resistance than the matrix alloy.

Conflicts of Interest

The author declares no conflicts of interest regarding the publication of this paper.

References

[1] Hemanth, J. (1996) Wear Characteristics of Sub Zero Chilled Cast Iron. *Wear*, **192**, 134-143. https://doi.org/10.1016/0043-1648(95)06781-7

[2] Hemanth, J. (1998) Effect of Cooling Rate on the Dendrite Arm Spacing and Ultimate Tensile Strength of Cast Iron. *Material Science*, **33**, 23-35.

[3] Hemanth, J. (2003) Effect of High Rate of Heat Transfer during Solidification of Alloyed Cast Iron Using Water-Cooled and Sub-Zero Chills on Mechanical Behavior. *Materials and Design*, **24**, 37-45. https://doi.org/10.1016/S0261-3069(02)00086-9

[4] Hemanth, J. (2007) Cryogenic Effects during Solidification on the Wear Behavior of Al Alloy/Glass CNMMCs. *Journal of Composite Materials Part A*, **38**, 1395-1402. https://doi.org/10.1016/j.compositesa.2006.09.007

[5] Hemanth, J. (2010) Microstructure, Mechanical Properties and Wear Behavior of Metallic, Nonmetallic and Deep Cryogenically Chilled ASTM a216 WCB Steel. *Journal of Alloys and Compounds*, **506**, 557-652. https://doi.org/10.1016/j.jallcom.2010.07.036

[6] Schueller, R.D. and Wawner, F.E. (1991) An Analysis of High-Temperature Behavior of AA2124/SiC Whisker Composites. *Composites Science and Technology*, **40**, 213-223. https://doi.org/10.1016/0266-3538(91)90098-A

[7] Scott, V.D. (1991) Interface Microstructures in Fibre-Reinforced Aluminium Alloys. *Composites Science and Technology*, **42**, 251-273. https://doi.org/10.1016/0266-3538(91)90020-P

[8] Bhagat, R.B. and Srinivasl, K. (1992) Elevated Temperature Strength, Aging Response and Creep of Aluminum Matrix Composites. *Journal of Composite Materials*, **26**, 1578-1593. https://doi.org/10.1177/002199839202601102

[9] Jansson, S. and Leckie, F.A. (1992) Reduction of Thermal Stresses in Continuous Fiber Reinforced Metal Matrix Composites with Interface Layers. *Journal of Composite Materials*, **26**, 1474-1486. https://doi.org/10.1177/002199839202601005

[10] Kindl, B., Grover, A. and Stanley, P. (1992) The Control of Interface and Microstructure of SiC/Al Composites by Sol-Gel Technique. *Composites Science and Technology*, **43**, 85-93. https://doi.org/10.1016/0266-3538(92)90135-P

[11] Lee, S. (1992) Thermal Effective Stress Concentration Problems in Metal Composites. *Composites Science and Technology*, **44**, 71-76. https://doi.org/10.1016/0266-3538(92)90026-Y

[12] Rozak, G.A. and Garner, H.J. (1992) Effect of Casting Conditions and Deformation Processing on A356 Aluminum and A356-20 % SiC Composites. *Journal of Composite Materials*, **26**, 2076-2106. https://doi.org/10.1177/002199839202601405

[13] Chen, F., Chen, Z., Mao, F., Wang, T. and Cao, Z. (2015) TiB 2 Reinforced Aluminum Based *in Situ* Composites Cast by Stir Casting. *Materials Science and Engineering A*, **625**, 357-368. https://doi.org/10.1016/j.msea.2014.12.033

[14] Saravanan, C., Subramanian, K., Ananda Krishnan, V. and Sankara Narayanan, R. (2015) Effect of Particulate Reinforced Aluminum Metal Matrix Composite—A Review. *Mechanics and Mechanical Engineering*, **19**, 23-30.

[15] Mohammadpour, M., Azari Khosroshahi, R., Taherzadeh Mousavian, R. and Brabazon, D. (2016) A Novel Method for Incorporation of Micron-Sized SiC Particles into Molten Pure Aluminum Utilizing a Co Coating. *Metallurgical and Materials Transactions B*, **46**, 12-19. https://doi.org/10.1007/s11663-014-0186-9

[16] Hemanth, J. (2018) Fabrication and Corrosion Behavior of Al-Alloy (LM-13) Reinforced with Nano-ZrO_2 Particulate Chilled Nano MMCs for Aerospace Applications. *Journal of Materials Science and Chemical Engineering*, **6**, 136-150. https://doi.org/10.4236/msce.2018.67015

[17] Akbari, M.K., Baharvandi, H.R. and Shirvanimoghaddam, K. (2015) Tensile and Fracture Behavior of Nano/Micro TiB 2 Particle Reinforced Casting A356 Aluminum Alloy Composites. *Materials & Design*, **66**, 150-161. https://doi.org/10.1016/j.matdes.2014.10.048

[18] Yamamoto, T., Sasamoto, H. and Inagaki, M. (2000) Extrusion of Al Based Composites. *Journal of Materials Science Letters*, **19**, 1053-1064. https://doi.org/10.1023/A:1006747305264

[19] Awasthi, S. and Wood, J.L. (1988) Mechanical Properties of Extruded Ceramic Reinforced Al Based Composites. *Advanced Ceramic Materials*, **35**, 3449-3458.

[20] Yeh, N.-M. and Krempl, E. (1992) A Numerical Simulation of the Effects of Volume Fraction, Creep and Thermal Cycling on the Behavior of Fibrous Metal-Matrix Composites. *Journal of Composite Materials*, **26**, 900-915. https://doi.org/10.1177/002199839202600607

[21] Chen, R. and Li, X. (1993) A Study of Silica Coatings on the Surface of Carbon or Graphite Fiber an the Interface in a Carbon/Magnesium Composite. *Composites Science and Technology*, **49**, 357-362. https://doi.org/10.1016/0266-3538(93)90067-Q

[22] Chen, R. and Zhang, G. (1993) Casting Defects and Properties of Cast A356 Aluminum Alloy Reinforced with SiC Particles. *Composites Science and Technology*, **47**, 51-56. https://doi.org/10.1016/0266-3538(93)90095-X

[23] Durrant, G. and Scott, V.D. (1993) The Effect of Forging on the Properties and Microstructure of Saffilfibre Reinforced Aluminum. *Composites Science and Technology*, **49**, 153-164. https://doi.org/10.1016/0266-3538(93)90055-L

[24] Komai, K. and Sinoy (1993) Tensile and Fatigue Fracture Behavior and Water-Environment Effects in a SiC-Whisker/7075-Aluminum Composite. *Composites Science and Technology*, **46**, 59-66. https://doi.org/10.1016/0266-3538(93)90081-Q

[25] Kun, Y. (1993) CVD SiC/Al Composites Produced by a Vacuum Suction Casting Process. *Composites Science and Technology*, **46**, 1-6. https://doi.org/10.1016/0266-3538(93)90075-R

[26] Samuel, A.M., Keren, A. and Lambo, L. (1993) On the Castability of Al-Si/SiC Particle-Reinforced Metal Matrix Composites: Factors Affecting Fluidity and Soundness. *Composites Science and Technology*, **49**, 1-12.

https://doi.org/10.1016/0266-3538(93)90016-A

[27] Assar, A.E.M. and Al-Nimr, M.D.A. (1994) Fabrication of Metal Matrix Composite by Infiltration Process Part 1: Modeling of Hydrodynamic and Thermal Behavior. *Journal of Composite Materials*, **28**, 1480-1490. https://doi.org/10.1177/002199839402801506

[28] Kang, C.G. and Ku, G.S. (1995) An Experimental Investigation on Infiltration Limit and the Mechanical Properties of Al_2O_3 Short Fiber Reinforced Metal Matrix Composites Cast by Squeeze Casting. *Journal of Composite Materials*, **29**, 444-462. https://doi.org/10.1177/002199839502900402

[29] Ananth, R. and Chandra, N. (1995) Numerical Modeling of Fiber Push-Out Test in Metallic and Intermetallic Matrix Composites-Mechanics of the Failure Process. *Journal of Composite Materials*, **29**, 1488-1514. https://doi.org/10.1177/002199839502901105

[30] Liu, X. and Bathias, C. (1993) Defects in Squeeze-Cast Al_2O_3/Al Alloy Composites and Their Effects on Mechanical Properties. *Composites Science and Technology*, **46**, 245-252. https://doi.org/10.1016/0266-3538(93)90158-D

[31] Anson, L.W. (1995) On the Feasibility of Detecting Pre-Cracking Fatigue Damage in Metal-Matrix Composites by Ultrasonic Techniques. *Composites Science and Technology*, **55**, 63-73. https://doi.org/10.1016/0266-3538(95)00088-7

[32] Begley, M.R. and McMeeking, R.M. (1995) Fatigue Crack Growth with Fiber Failure in Metal-Matrix Composites. *Composites Science and Technology*, **53**, 365-382. https://doi.org/10.1016/0266-3538(95)00009-7

[33] Canumalla, S. and Barnard, J. (1995) Mechanical Behavior of Mullite Fiber Reinforced Aluminum Alloy Composites. *Journal of Composite Materials*, **29**, 653-670. https://doi.org/10.1177/002199839502900506

[34] Chandra, N. and Ananth, C.R. (1995) Analysis of Interfacial Behavior in MMCs and IMCs by the Use of Thin-Slice Push-Out Tests. *Composites Science and Technology*, **54**, 87-100. https://doi.org/10.1016/0266-3538(95)00040-2

[35] Hemanth, J. (2011) Development and Wear Behavior of Al/Al2SiO5/C Chilled Hybrid Metal Matrix Composites by both Experimental and Finite Element Method. SAE International, Warrendale, Paper No. 2011-01-0223. https://doi.org/10.4271/2011-01-0223

[36] Anilkumar, A. and Anilkumar, C. (2014) Studies on Mechanical, Wear and Corrosion Properties of Al6061-Beryl-Cerium Oxide Hybrid MMCs. *International Journal of Research in Engineering and Technology*, **3**, 23-29. https://doi.org/10.15623/ijret.2014.0306042

[37] Xu, C., Zhang, Y., Wu, G., Wang, X. and Zhang, H. (2010) Rare Earth Ceramic Cutting Tool and Its Cutting Behavior When Machining Hardened Steel and Cast Iron. *Journal of Rare Earth*, **28**, 492-501. https://doi.org/10.1016/S1002-0721(10)60318-3

[38] Wu, T., Zhou, J., Wu, B. and Li, W. (2016) Effect of La_2O_3 Content on Wear Resistance of Alumina Ceramics. *Journal of Rare Earth*, **34**, 288-295. https://doi.org/10.1016/S1002-0721(16)60027-3

[39] Sajjadi, S.A., Ezatpour, H.R. and Beygi, H. (2011) Microstructure and Mechanical Properties of Al-Al_2O_3 Micro and Nano Composites Fabricated by Stir Casting. *Materials Science and Engineering*: *A*, **528**, 8765-8771. https://doi.org/10.1016/j.msea.2011.08.052

[40] Surappa, M.K. (2003) Aluminum Matrix Composites: Challenges and Opportunities. *Sadhana*, **28**, 319-334. https://doi.org/10.1007/BF02717141

[41] Veeresh Kumar, G.B., Rao, C.S.P. and Selvaraj, N. (2011) Mechanical and Tribological Behavior of Particulate Reinforced Aluminum MMCs—A Review. *Journal of Minerals & Materials Characterization & Engineering*, **10**, 59-91. https://doi.org/10.4236/jmmce.2011.101005

[42] Hemanth, J. (2010) Microstructure, Mechanical Properties and Wear Behavior of Metallic, Nonmetallic and Deep Cryogenically Chilled ASTM a216 WCB Steel. *Journal of Alloys and Compounds*, **506**, 557-652. https://doi.org/10.1016/j.jallcom.2010.07.036

[43] Hemanth, J. (2011) Abrasive and Slurry Wear Behavior of Chilled Aluminum Alloy (A356) Reinforced with Fused Silica (SiO_{2p}) MMCs. *Composites Part B*, **42**, 1826-1833. https://doi.org/10.1016/j.compositesb.2011.06.022

[44] Hemanth, J. and Steevanson, S.S. (2019) Corrosion and Wear Behavior of Nano-Zr Coated Commercial Grade Cast Iron by Sol-Gel and Plasma Spray Process. *Open Journal of Composite Materials*, **9**, 57-71. https://doi.org/10.4236/ojcm.2019.92003

[45] Sample, R.J. and Kevein, W.B. (1989) High Pressure Squeeze Casting of Unidirectional Graphite Fiber Reinforcedaluminum Matrix Composites. *Journal of Composite Materials*, **23**, 1021-1028. https://doi.org/10.1177/002199838902301005

[46] Stanford-Beale, C.A. and Clyne, T.W. (1989) Extrusion and High-Temperature Deformation of Fibre-Reinforced Aluminum. *Composites Science and Technology*, **35**, 121-157. https://doi.org/10.1016/0266-3538(89)90092-4

[47] Wu, J.F. and Zing Lu, P.S. (1989) A Material Model for the Finite Element Analysis of Metal Matrix Composites. *Composites Science and Technology*, **35**, 347-366. https://doi.org/10.1016/0266-3538(89)90057-2

[48] Xiong, Z. and Xiu, K. (1990) Investigation of High-Temperature Deformation Behavior of a SiC Whisker Reinforced 6061 Aluminum Composite. *Composites Science and Technology*, **39**, 117-125. https://doi.org/10.1016/0266-3538(90)90050-F

[49] Iwai, Y. and Honda, H. (1995) Sliding Wear Behavior of SiC Whisker Reinforced Al Composites. *Wear*, **181**, 594-602. https://doi.org/10.1016/0043-1648(95)90175-2

[50] Wang, A. and Rack, H.J. (1991) Friction Behavior of Al-SiCp Composites. *Wear*, **146**, 337-344. https://doi.org/10.1016/0043-1648(91)90073-4

[51] Mondal, D.P., Das, S. and Jha, A.K. (1998) Abrasion Wear of Al Based Composites. *Wear*, **223**, 131-139. https://doi.org/10.1016/S0043-1648(98)00278-6

[52] Wang, A.G. and Hutchings, I.M. (1989) Wear of Alumina-Fibre Aluminum Composites. *Materials Science and Technology*, **5**, 71-84. https://doi.org/10.1179/026708389790337503

[53] Moustafa, S.F. (1995) Wear and Wear Mechanism of Al-22%Si/Al_2O_3 Composites. *Wear*, **95**, 185-198. https://doi.org/10.1016/0043-1648(95)06607-1

[54] Moore, M.A. and Douthwaite, R.M. (1976) Tribological Behavior of Ceramic Based Composites. *Metallurgical and Materials Transactions A*, **7**, 1833-1842. https://doi.org/10.1007/BF02654978

[55] Prasad, B.K., Modi, O.P. and Jha, A.K. (1994) Metallurgical Aspects of Al Based Composites. *Tribology International*, **27**, 153-158. https://doi.org/10.1016/0301-679X(94)90039-6

[56] Prasad, B.K., Das, S. and Jha, A.K. (1997) Dry Sliding Wear of Al Based Composites. *Composites Part A*, **28**, 301-309. https://doi.org/10.1016/S1359-835X(96)00115-7

[57] Meng, F. and Tagashira, K. (1994) Wear Resistance and Microstructure of Cryogenic Treated Fe-1.4Cr-1C Bearing Steel. *Scripta Metallurgica et Materialia*, **7**, 865-873.

https://doi.org/10.1016/0956-716X(94)90493-6

[58] Bensely, A., Prabhakaran, A., MohanLal, D. and Nagarajan, G. (2006) Enhancing the Wear Resistance of Case Carburized Steel (En353) by Cryogenic Treatment. *Cryogenics*, **45**, 747-754. https://doi.org/10.1016/j.cryogenics.2005.10.004

[59] Zhang, J. and Alpas, A.T. (1993) Wear Regimes and Transition in Al_2O_3 Particulate Composites. *Materials Science and Engineering*: *A*, **161**, 273-280. https://doi.org/10.1016/0921-5093(93)90522-G

[60] Venkataraman, B. and Sundarajan, G. (1996) The Sliding Wear Behavior of Al-SiC Particulate Composites. *Acta Materialia*, **44**, 451-462. https://doi.org/10.1016/1359-6454(95)00217-0